Bulletin of the Seismological Society of America. Vol. 64, No. 5, pp. 1477–1499. October 1974

MICROEARTHQUAKE DISTRIBUTION AND MECHANISMS OF FAULTING IN THE FONTANA-SAN BERNARDINO AREA OF SOUTHERN CALIFORNIA

BY DAVID HADLEY* AND JIM COMBS†

ABSTRACT

The major, historically active San Jacinto and San Andreas fault systems pass through the San Bernardino Valley area of southern California. An array of six portable, high-gain seismographs was operated for five 2-week recording sessions during the summer of 1972 and winter and spring of 1973 in order to detail the microseismicity of the region. A crustal model for the Valley, modified after Gutenberg, was established using a 6-km reversed seismic refraction profile and a series of monitored quarry blasts. Fifty-five microearthquakes were used to establish a magnitude scale (1.5 to 3.3) based on coda lengths recorded by instruments peaked at 20 Hz. Forty-five hypocenters from the analysis of over 6,000 hr of low-noise records define two northeast trending lineations within the western portion of the Valley. A composite first-motion plot of 22 microearthquakes from these lineations indicates left-lateral strike-slip faulting. Fluctuations in microseismicity appear to reflect rapid changes in the stress patterns of southern California. Minor activity along the strike of the San Jacinto fault zone suggests a purely right-lateral strike-slip motion. Only minimal strain release was observed along the San Andreas fault zone.

INTRODUCTION

The San Bernardino Valley area is one of the major inland alluvial basins in southern California. Common usage of the term "the San Bernardino Valley" implies only that portion of the upper Santa Ana Basin east of the San Jacinto fault. In this study the term "San Bernardino Valley area", sometimes referred to as the "Valley", has been expanded to include all of the stippled area shown in Figure 1.

The San Andreas and the San Jacinto faults have been the focal points of destructive earthquakes in southern California within historical times (Richter, 1958; Allen, *et al.*, 1965). Both faults crosscut the San Bernardino Valley. Inasmuch as the area has received little detailed seismic investigation, an array of six portable seismographs was operated in and around the San Bernardino Valley during the summer of 1972 and winter and spring of 1973. Initially, a large array was established to delineate the seismically active areas; but, a tighter net was utilized in the final recording period to define more accurately the zones of faulting and the sense of motion. Over 6,000 hr of low-noise records were accumulated and analyzed.

STRUCTURE AND GENERAL GEOLOGY

The structure and geological relationship in the San Bernardino Valley are severely complicated by large-scale regional tectonics. Four distinct blocks of the Earth's crust can be identified within the Valley, each in relative motion with respect to the others. The Perris block is bound on the east and north by the San Jacinto and the Cucamonga fault zones, respectively (Dudley, 1936; see Figure 2). Outlined by the San Jacinto and

*Present address: Seismological Laboratory, California Institute of Technology, Pasadena, California 91109.

†Present address Institute for Geosciences, University of Texas at Dallas, P.O. Box 688, Richardson, Texas 75080.

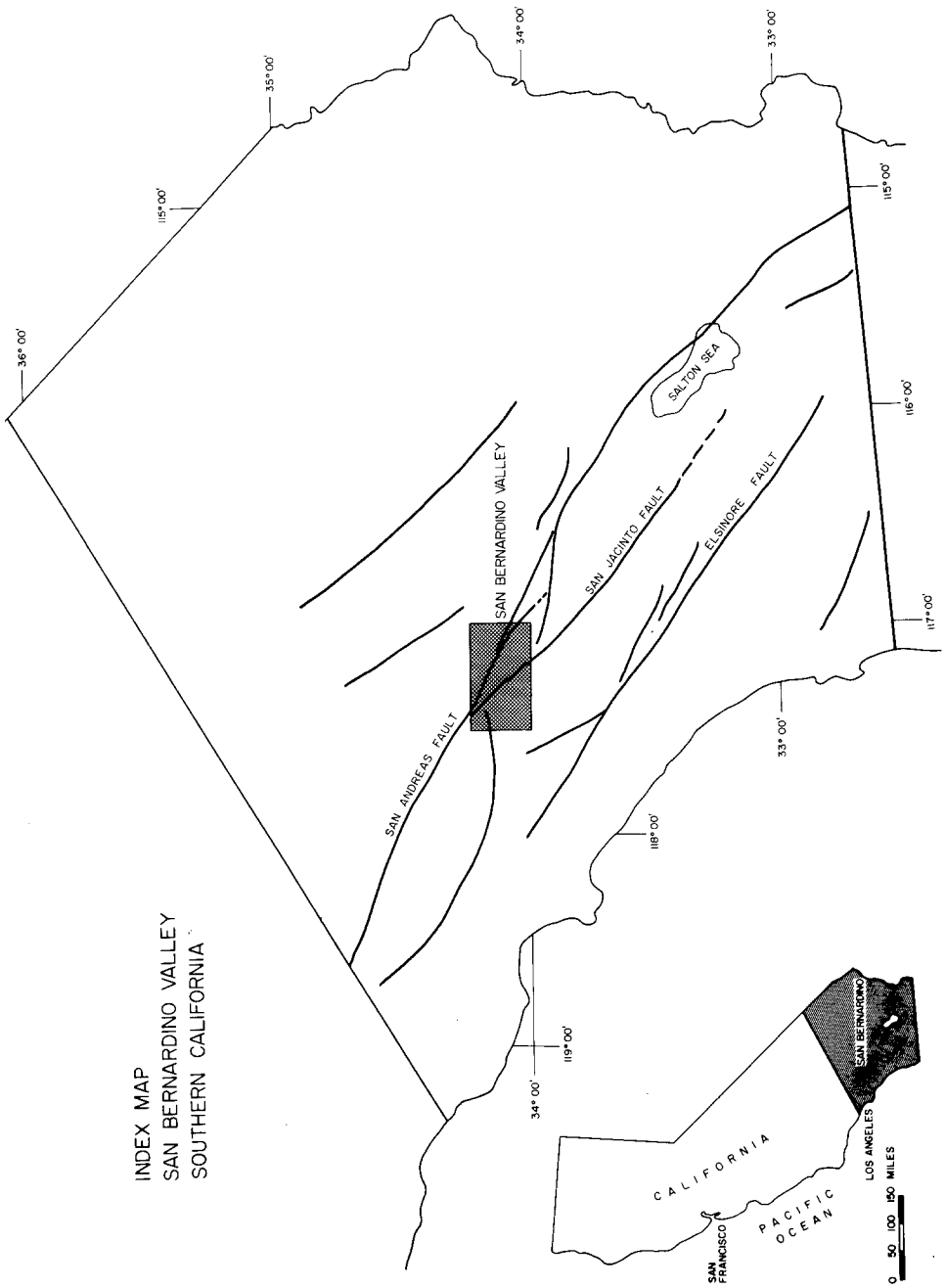

FIG. 1. Index map: Stippled rectangle depicts the San Bernardino Valley area of southern California.

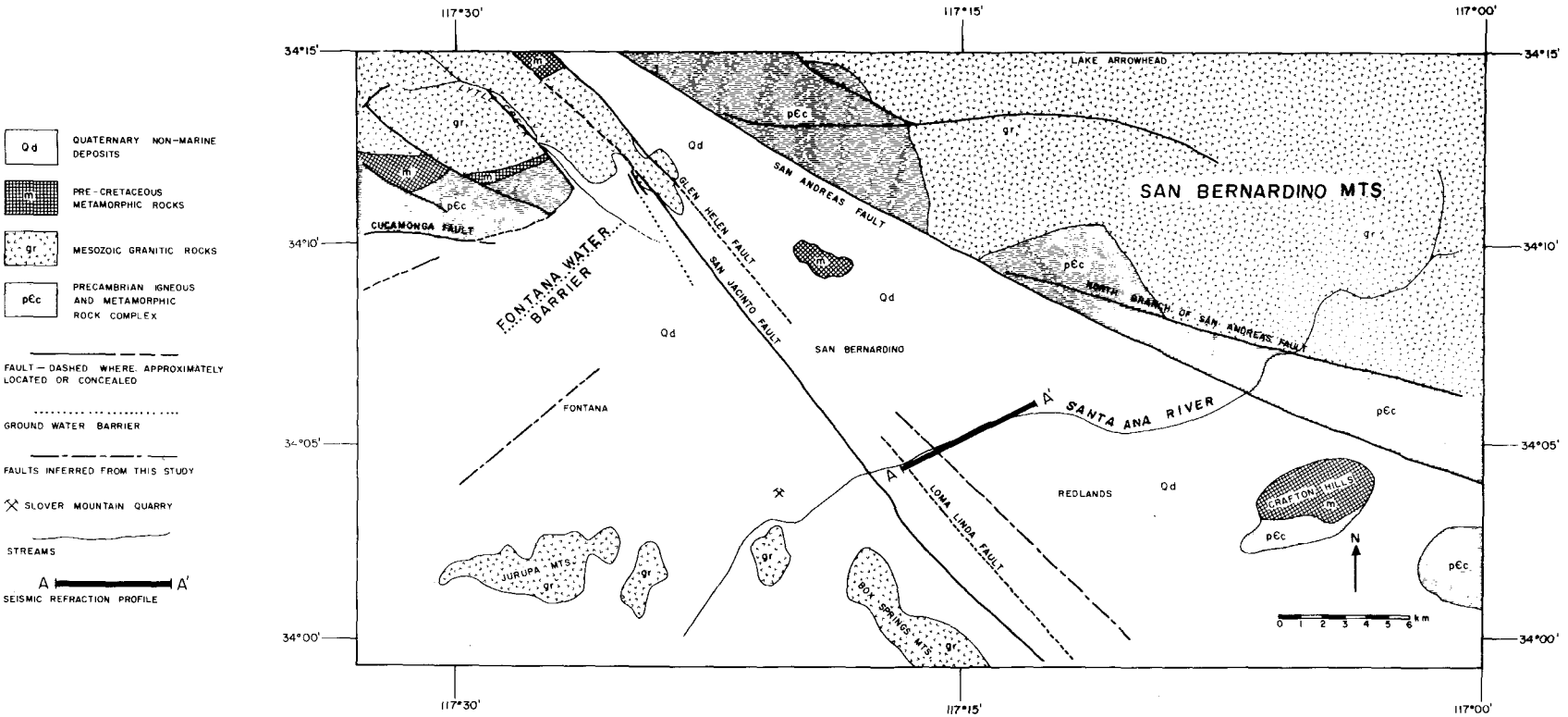

FIG. 2. Generalized geological map of the San Bernardino Valley area (after, Rogers, 1967).

the San Andreas faults, a wedge of the San Jacinto block forms the eastern portion of the Valley. The San Gabriel and the San Bernardino Mountains form the eastern portion of the Transverse Ranges (Allen, *et al.*, 1965). The San Gabriel block, rising sharply from the northwest side of the San Bernardino Valley, is marked by irregular, broken terrain that locally reaches elevations of 3 km (Dutcher and Garrett, 1963). The San Bernardino Mountains, forming the northern edge of the basin, are characterized by a very regular crest. The general topographic uniformity of this block as compared to the dissected San Gabriel block suggests a relatively recent uplift. The northern branch of the San Andreas fault splays from the main fracture system and transects the southern portion of the San Bernardino Mountains (Dibblee, 1968). Allen (1957) has reported both horizontal and vertical slickensides within this fault zone but attributes the greater average northern elevation to the fault. The currently inactive east-west trending Banning fault (Dibblee, 1968) is located southeast of the San Bernardino Valley, and its western extent is covered by undisturbed Pleistocene alluvial sediments. Both Allen (1957) and Sharp (1967) have suggested that the Cucamonga fault is the western extension of the Banning fault, displaced 25 km north by the San Jacinto fault. The Loma Linda fault (Figure 2) parallels the San Jacinto fault zone. Dutcher and Garrett (1963) report there is no evidence of recent movement upon the Loma Linda fault within the basin, as displaced units are buried 30 meters beneath apparently undisturbed sediments. Water-well logs indicate faulting extended into the Valley. Because the Glen Helen fault lies on strike, Dutcher and Garrett (1963) suggested these two faults are possibly continuous beneath the recent accumulation of sediments.

The San Jacinto fault forms a major structural feature throughout southern California and is the most active, both in terms of major historical earthquakes and on-going microearthquake activity (Arabasz, *et al.*, 1970; Cheatum and Combs, 1973). Within the San Bernardino Valley there appears to be little, if any, vertical offset associated with the fault. Unlike the Loma Linda fault zone, surface sediments along the San Jacinto fault have been disrupted suggesting recent movement.

The east-trending Cucamonga fault is truncated by the San Jacinto fault zone. Dutcher and Garrett (1963) report minor thrusting on a plane dipping 40° north along a portion of the Cucamonga fault. A water barrier 4 km to the south trends approximately north-easterly (Dutcher and Garrett, 1963) and will be termed for convenience the Fontana Water Barrier (see Figure 2).

Several minor bedrock hills surround the Valley. Small knolls in the northern portion of the Valley are possibly associated with faulting in the basement complex. The more southern Jurupa and Box Springs Mountains (Figure 2) represent the northern outcropping of the southern California batholith (Dudley, 1936).

Previous Investigations

One station in the microearthquake survey ($0 < M < 3$) of southern California conducted by Brune and Allen (1967) was located within the San Bernardino Valley. Over 1,000 hr of useful records from their Devil Canyon station indicate an average of six microearthquakes per day within a radius of 24 km. A station operated in Devil Canyon during the present study indicates a similar number of events per day. As part of their 1967 study, Brune and Allen operated a five-station array for 4 months slightly north of Lytle Creek. Five of 23 events they located were within the Fontana area of the San Bernardino Valley.

Earthquakes monitored by the California Institute of Technology provide data on the tectonic activity within the Valley. The northwestern cluster of events seen in Figure

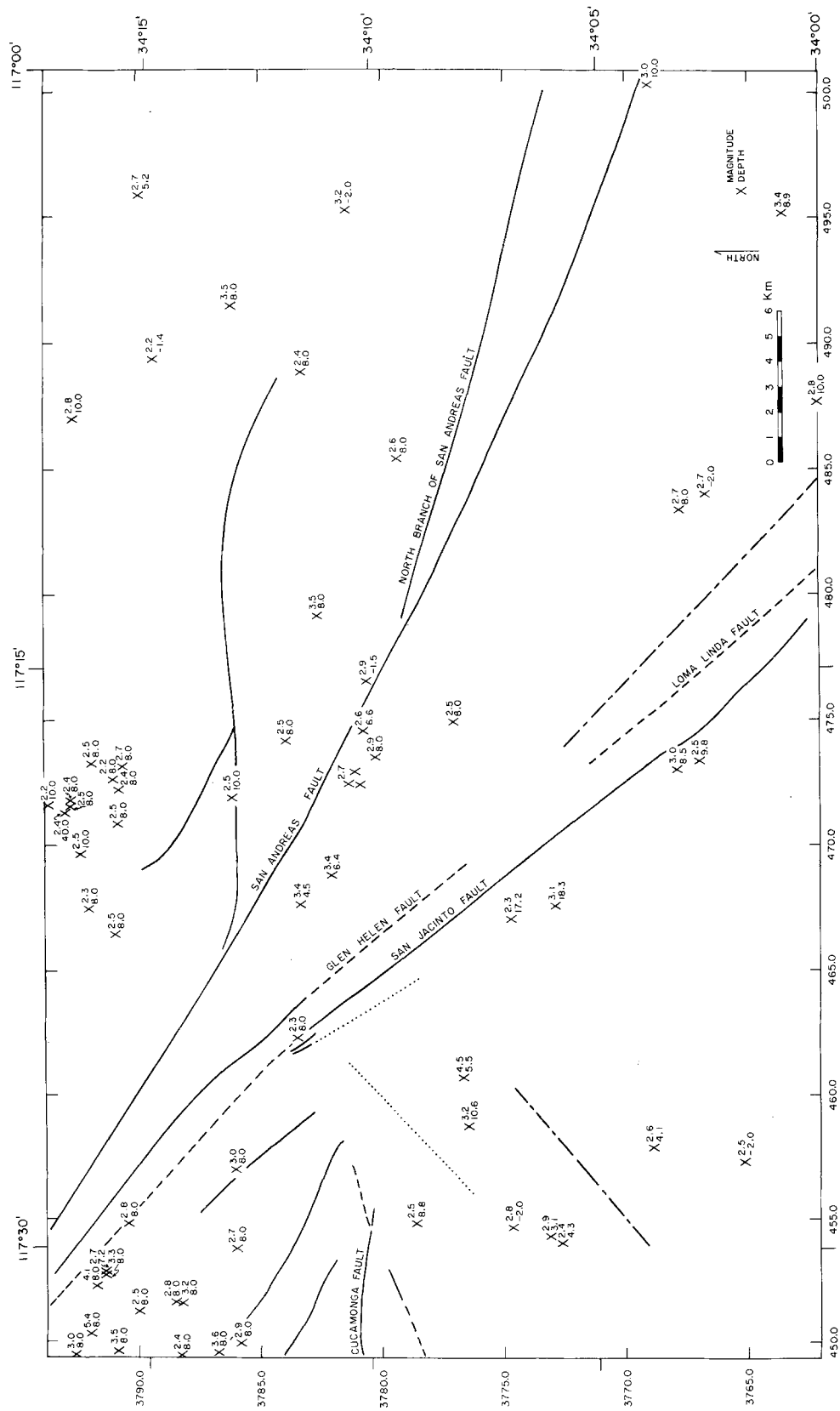

FIG. 3. Earthquake epicenters located with the California Institute of Technology Seismological Network, 1962–1970. The upper number is the magnitude and the lower one is the focal depth in kilometers. The Universal Transverse Mercador coordinates for the Valley are shown on the *left* and *lower* margins of the figure.

3 are aftershocks from the magnitude 5.4 Lytle Creek earthquake of 1970. During the 9-year period illustrated, an average of only one earthquake per year, with $M < 3.5$, was associated with the San Andreas fault within the Valley. As in Brune and Allen's (1967) study, shallow hypocenters are found within the Fontana area. Based on historical data, Allen (1968) suggests that the San Bernardino Valley area has been characterized by small to moderate earthquakes but devoid of truly great earthquakes such as the magnitude 8.3 San Francisco earthquake of April 18, 1906. The largest event in historical times within the Valley was a magnitude 6.2 earthquake of 1923 located approximately near the Box Springs Mountains (Richter, 1958).

Instrumentation

Six portable Kinemetrics PS-1 recording units, described in detail by Prothero and Brune (1971), were used for this study. Several different filters provided with the seismographs can be used to shape the system response (see Figure 4). Filter 1, peaked at 1 Hz, produced easily discernible first motions although it may have reduced the number of

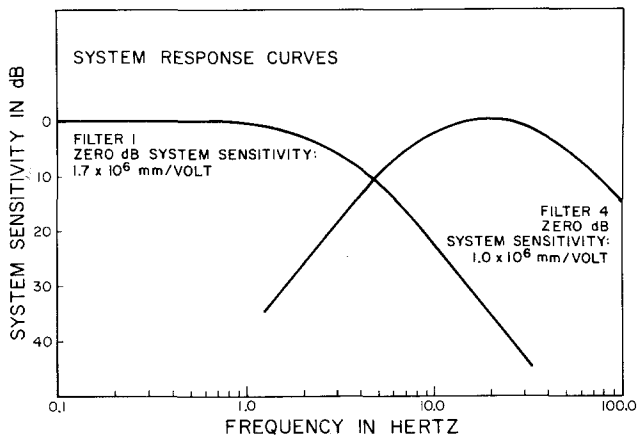

FIG. 4. Response curves for system used in present study.

small microearthquakes that were recorded. A higher resolution of events and well-defined $S-P$ intervals were obtained by using filter 4, peaked at 20 Hz which is the predominant frequency for very near microearthquakes. Gain is controlled by attenuating the maximum system sensitivity in 6-db steps. Stations operated on filter 4 were usually attenuated from 24 to 36 db, whereas the same stations could be operated on filter 1 with approximately 12 db less attenuation. Recording at 1 mm/sec was done with both ink and smoked paper systems. Inking on tracing paper proved to be the most suitable method for ease in correlating events from various stations. Some representative records using both filters 1 and 4 are presented in Figure 5.

Ranger type seismometers with a natural frequency of 1 Hz were used. The average generator constant for them was 100 V·sec/m. External resistors damped the system at 0.7 critical.

Timing for the recording units was provided by a temperature-compensated, crystal-controlled unit with an accuracy of ± 0.3 ppm over the temperature range of 0°C to 50°C. Timing was re-established at each station each day using the National Bureau of Standards WWV broadcast system.

The drum speed and the accurate timing allowed *P* arrivals to be picked to 0.1 sec. Using filter 4, *S* arrivals could often be picked with similar accuracy and were routinely used in the location of events.

Crustal Model

Several major problems are associated with the accurate location of events within the San Bernardino Valley. A reversed seismic refraction profile (Figure 2 and Figure 6) was shot in the course of this study in order to determine the depth to basement and a velocity model for the shallow subsurface portion of the basin. The overburden was found to consist of three zones with average thicknesses of 40, 300, and 670 meters and

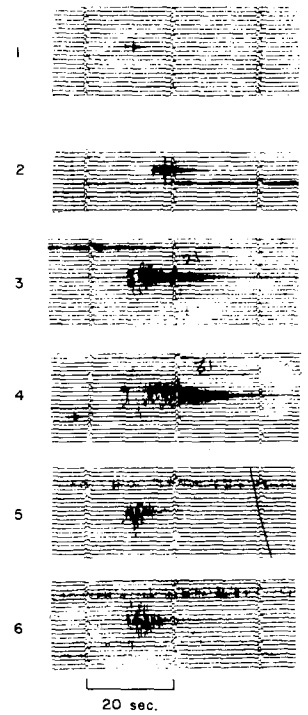

FIG. 5. Representative microearthquakes recorded with the seismic packs peaked at 20 Hz, events 1 through 4, and, at 1 Hz, events 5 and 6. Note the well-defined *P* and *S* arrivals in events 1 and 2. The signal duration of events 3 and 4 was measured as 21 and 31 sec, respectively. Clear first motions can be seen in events 5 and 6. Recording was done at 60 mm/sec.

with corresponding seismic velocities of 0.67, 2.0, and 2.9 km/sec (see Figure 6). The depth of penetration and recorded velocity suggests that at least the upper 1 km of the basement complex of the San Jacinto block within the Valley is characterized by a low velocity (5.3 km/sec).

Quarry blasts monitored at Slover Mountain (see Figure 2) and recorded around the Valley indicate that the upper portions of the Perris block have a seismic velocity of approximately 5.8 km/sec. Several different layered velocity models were used in an attempt to average this velocity contrast; however, gross changes in the models seldom changed horizontal locations by more than 5 km. Because most of the recording sites were located on basement complex and most hypocenters appear to be deeper than 1 km, a modified version of Gutenberg's (1955) velocity model (Figure 7) was chosen as giving

the minimum residual travel times for most recorded microearthquakes. The low-velocity upper layer reflects the sediments in the Valley. The seismic velocity of the next two layers has been reduced from Gutenberg's model to correspond to the contribution of the San Jacinto block. At a depth of 16 km, the difference between the two blocks probably becomes insignificant and the model corresponds to Gutenberg's model.

The second problem concerns station delay times. Some stations were located on crystalline outcrops whereas others were on 500 to 800 meters of sedimentary and/or metamorphic rocks (see Table 1). Elevation contrasts between stations were as much as 500 meters. Station delay times were adjusted to correspond roughly to the geological and topographic corrections, that is, negative delays for lower elevations and crystalline

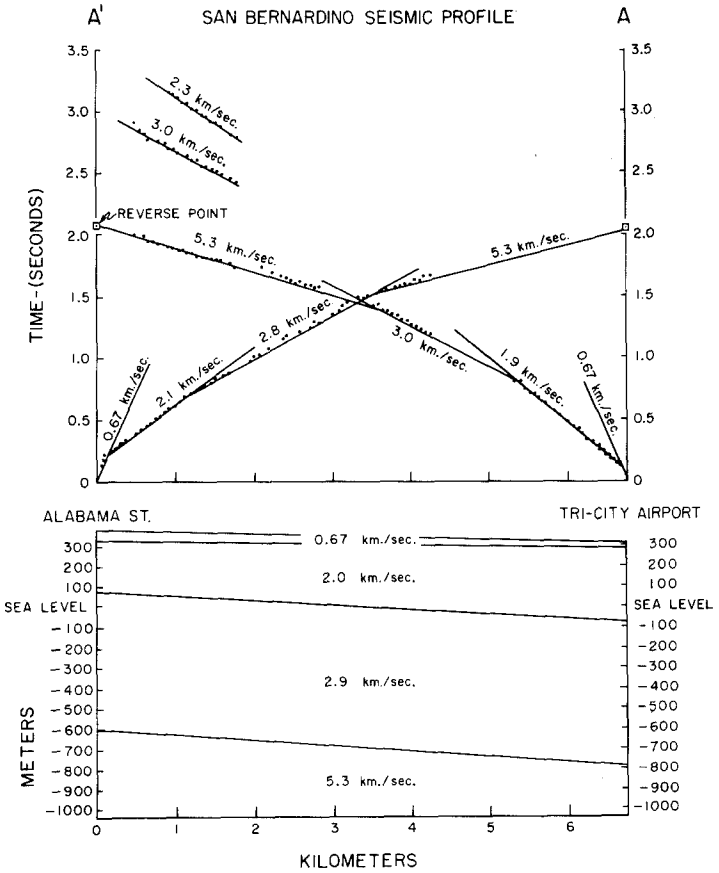

FIG. 6. Reversed seismic refraction profile. The exact location of the profile is illustrated in Figure 2.

outcrops and positive delays for higher elevations and thick sequences of sediments. Fine adjustments in the station delays were made on the basis of five quarry blasts at Slover Mountain (see Figure 2). The actual quarry blast locations and the computer locations are listed in Universal Transverse Mercator coordinates in Table 2. The average error for the blasts is 0.98 km in the horizontal plane and 0.27 km in depth. Two slightly different station arrays were used to record the five blasts. The majority of the located events within this study were recorded by the array typified by the February 1973 quarry blasts. The typical hypocentral uncertainties for located events are 1 km. Hypocentral location was determined by using a stepwise multiple regression computer program (Lee and Lahr, 1972). Detailed microearthquake and quarry blast reductions for this

study are presented in Hadley (1973). Greater than 60 per cent of the located events have rms residual travel times less than 0.1 sec and 80 per cent have less than 0.2 sec. The quality of location for events outside the array undoubtedly is not as great as for those within, the error increasing with distance.

Magnitudes

Magnitudes for the majority of the recorded events were determined on the basis of instrumental response (Eaton *et al.*, 1970). A computer program was written to calculate

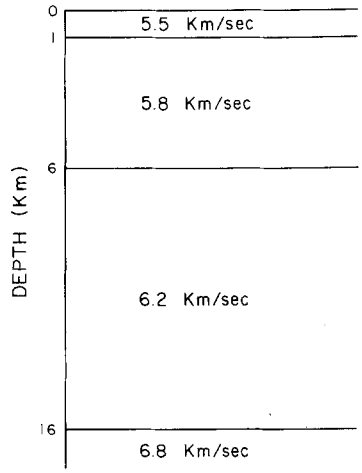

FIG. 7. Velocity model used for hypocenter location in present study, modified from Gutenberg (1955).

the actual ground motion within the frequency range of 0.5 to 4 Hz for each seismic pack. The expected response of the standard Wood-Anderson torsion seismometer was then calculated. Richter (1958) defined magnitude as

$$M = \log_{10}(A/A_0) \tag{1}$$

where A is the maximum record displacement in millimeters of the standard torsion seismometer and A_0 is the displacement for a magnitude zero event at the same distance. A similar expression is

$$M = \log_{10}G - \log_{10}A_0 + \log_{10}A' \tag{2}$$

where G is the observed ground motion and A' is the amplification of the Wood-Anderson seismograph. Calculated magnitudes for an event recorded at different stations varied by as much as 0.4. Hence, most magnitudes represent a simple average between two or more stations. As pointed out by Richter (1958), the maximum amplitude recorded on a standard torsion seismometer may not correlate with the maximum amplitude registered on instruments with a different frequency response. An attempt was made to avoid this problem and to provide a convenient method for quickly determining magnitudes. Based on 55 microearthquakes, an empirical relationship was found between the calculated magnitudes and the signal duration for events recorded at a peak response of 20 Hz (Figure 8).

Several empirical formulas have been derived by various authors. Using the Wakayama microearthquake network in Japan, Tsumura (1967) correlated the total duration of

TABLE 1

STATION DESCRIPTIONS

Location	Station	Latitude	Longitude	Dates Operated	Average Attenuation (db) Filter 1	Filter 4	Rock Type
W. Riverside	WRV1	34° 0.76′	117°26.81′	6/24/72–7/7/72 7/25/72–8/4/72	36*		Alluvium
Lytle Creek	LYCC	34°13.94′	117°28.96′	6/24/72–7/7/72 7/25/72–8/4/72	30*		Metasediments
City Creek	CCR3	34°11.20′	117°10.69′	6/24/72–7/7/72 7/25/72–8/4/72	30*		Granitic
Mill Creek	MLL1	34° 4.72′	117° 2.62′	6/24/72–7/7/72 7/25/72–8/4/72	36*		Alluvium
Box Springs	DREL	33°59.50′	117°18.95′	6/24/72–7/7/72 7/25/72–8/4/72	24*		Granitic
Jurupa Mts.	WRIV	34° 1.12′	117°24.90′	1/13/73–1/26/73 2/10/73–2/23/73 4/5/73–4/13/73	12	24	Granitic
Lytle Creek	LYCR	34°14.55′	117°28.43′	1/13/73–1/26/73 2/10/73–2/23/73	18	24	Metasediments
Bailey Canyon	BACN	34°12.65′	117°20.82′	1/16/73–1/20/73	30		Metasediments
Devil Canyon	DEVL	34°12.03′	117°19.32′	1/20/73–1/26/73 2/10/73–2/23/73 4/5/73–4/13/73	12	30	Metasediments
City Creek	CCR1	34°11.34′	117°11.36′	1/13/73–1/26/73	12	30	Granitic
Mill Creek	MILL	34° 6.20′	117° 1.60′	1/13/73–1/26/73	18	36	Metasediments
Box Springs	BOXS	33°59.65′	117°19.20′	1/14/73–1/26/73 2/10/73–2/23/73 4/5/73–4/13/73	12	30	Granitic
City Creek	CCR2	34°11.15′	117°10.88′	2/14/73–2/23/73	18		Granitic
Jurupa Mts.	JURU	34° 1.82′	117°29.90′	4/5/73–4/13/73	18		Granitic
Day Canyon	DAYC	34°11.05′	117°32.22′	4/5/73–4/13/73	12		Metasediments
Lytle Creek	LYC1	34°11.87′	117°25.85′	4/5/73–4/13/73	12	24	Granitic

*Seismometers damped at 0.1 critical.

TABLE 2

FIVE SLOVER MOUNTAIN QUARRY BLASTS USED TO REFINE VELOCITY MODEL USED IN HYPOCENTER LOCATIONS*

Date	Actual Location† UTM X	UTM Y	HYPO71 Location UTM X	UTM Y	Depth Error (km)	Horizontal Plane Error (km)	Rms‡	Charge Size (kg)
7/6/72	468.76	3768.85	467.67	3767.96	0.71	1.09	0.04	1100
7/7/72	469.02	3768.71	467.88	3768.50	0.17	1.16	0.03	1800
8/4/72	468.66	3768.95	468.18	3767.97	0.06	1.09	0.01	1450
2/15/73	468.65	3768.99	469.41	3769.79	0.19	1.10	0.22	2600
2/23/72	468.94	3768.82	468.49	3768.98	0.22	0.48	0.08	800

*The amount of average error is 0.98 km in the horizontal plane and 0.27 km in depth.

†All quarry blasts were approximately 0 km in depth.

‡Root mean square of the residual travel time in seconds.

oscillation, "$F-P$", with magnitude

$$M = -2.53+2.85 \log_{10}(F-P)+0.0014\Delta \quad (3)$$

where Δ is in kilometers. Working in the Puget Sound region and using instruments with a similar frequency response, Crosson (1972) found

$$M = -2.46+2.82 \log_{10}(F-P). \quad (4)$$

In a thorough study by Lee *et al.* (1972), 351 earthquakes from central California were used in determining

$$M = -0.87+2.0 \log_{10}(t)+0.0035\Delta \quad (5)$$

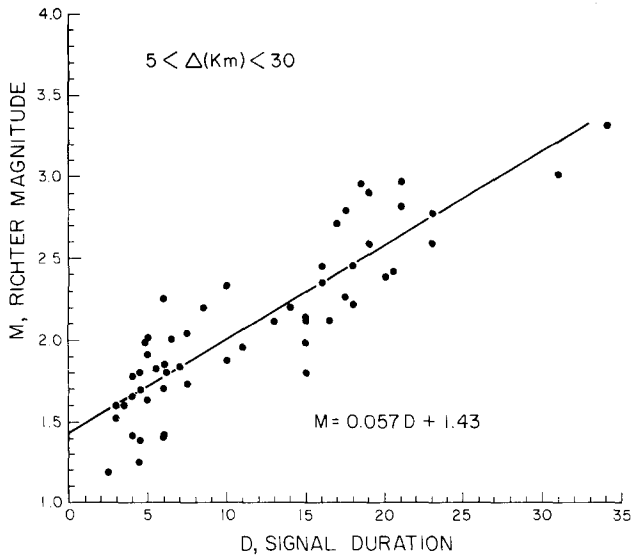

FIG. 8. Signal duration-magnitude relationship. Magnitudes represent the average of calculated magnitudes, based on system response of two or more stations peaked at 1 Hz. Duration of all events, recorded with a maximum gain of 20 Hz, was measured from the onset of the *P* arrival until the trace amplitude fell below 1 mm, or approximately a signal-to-noise ratio of 4:1. All duration measurements were made on records recorded at the West Riverside Station.

where t is the signal duration in seconds. In a more recent study along the Elsinore fault zone in southern California, Langenkamp (1973) and Langenkamp and Combs (1974) derived another relationship, that is,

$$M = -1.9+2.0 \log_{10}(t). \quad (6)$$

In order to compare the above correlations derived by these investigators a signal duration of 10 sec and an epicentral distance of 10 km were assumed. These assumptions for equations (3), (4), (5), and (6) lead to magnitudes of 0.33, 0.36, 1.16, and 0.1, respectively. Variables such as local geology, source and amplitude of background noise, frequency response of the systems, and methods of picking records probably accounts for this wide variation.

SEISMICITY

The epicentral positions of all microearthquakes located in this study are illustrated in Figure 9. The Fontana cluster of events is one of the most striking results of this study. As demonstrated by the plots of each recording session, Figures 10, 11, 12, and 13, this

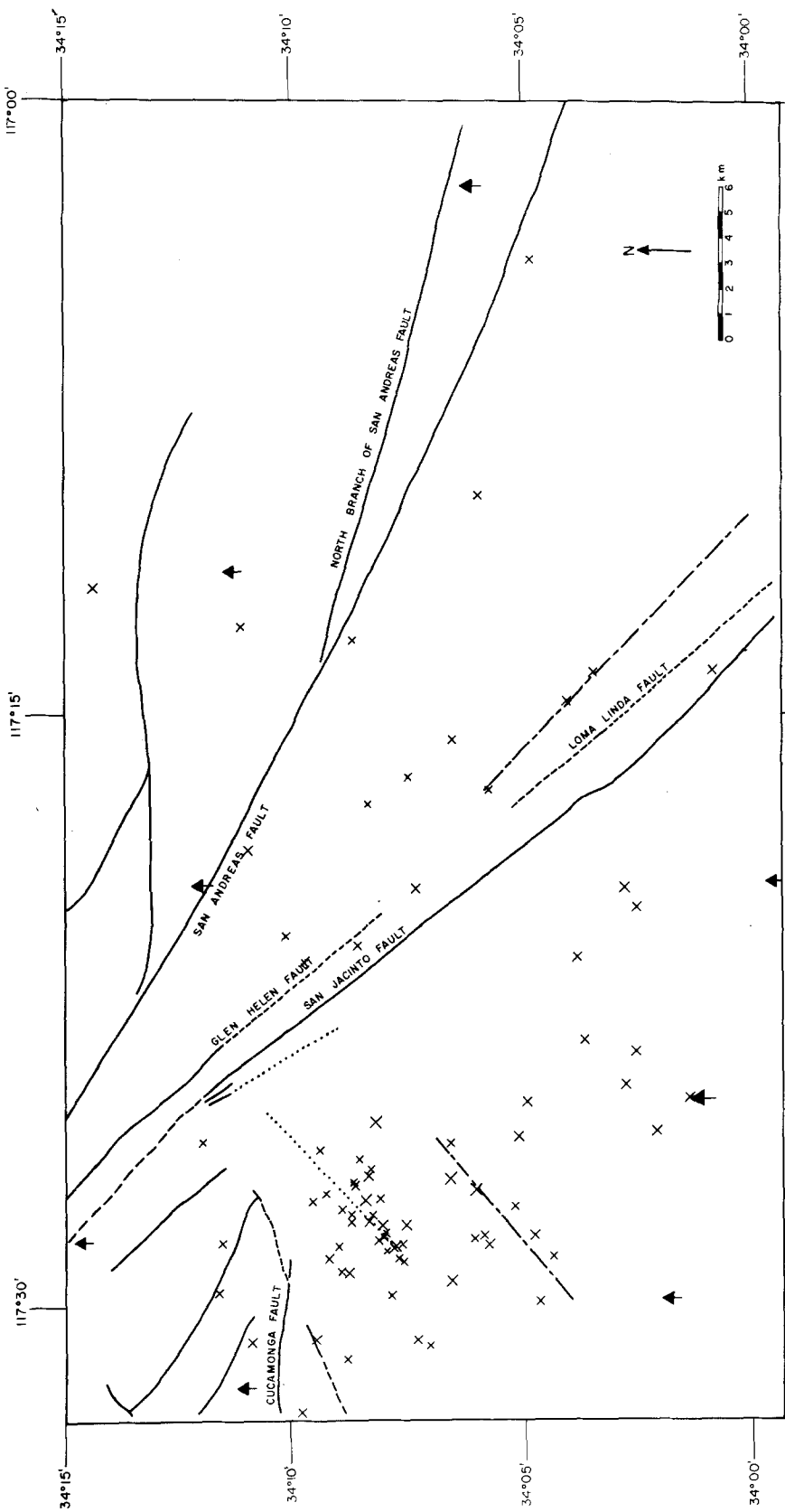

FIG. 9. All hypocenters of the San Bernardino earthquake of 1972 and 1973 located during this study. The size of the X is proportional to the magnitude. Only six recording stations were used at any time.

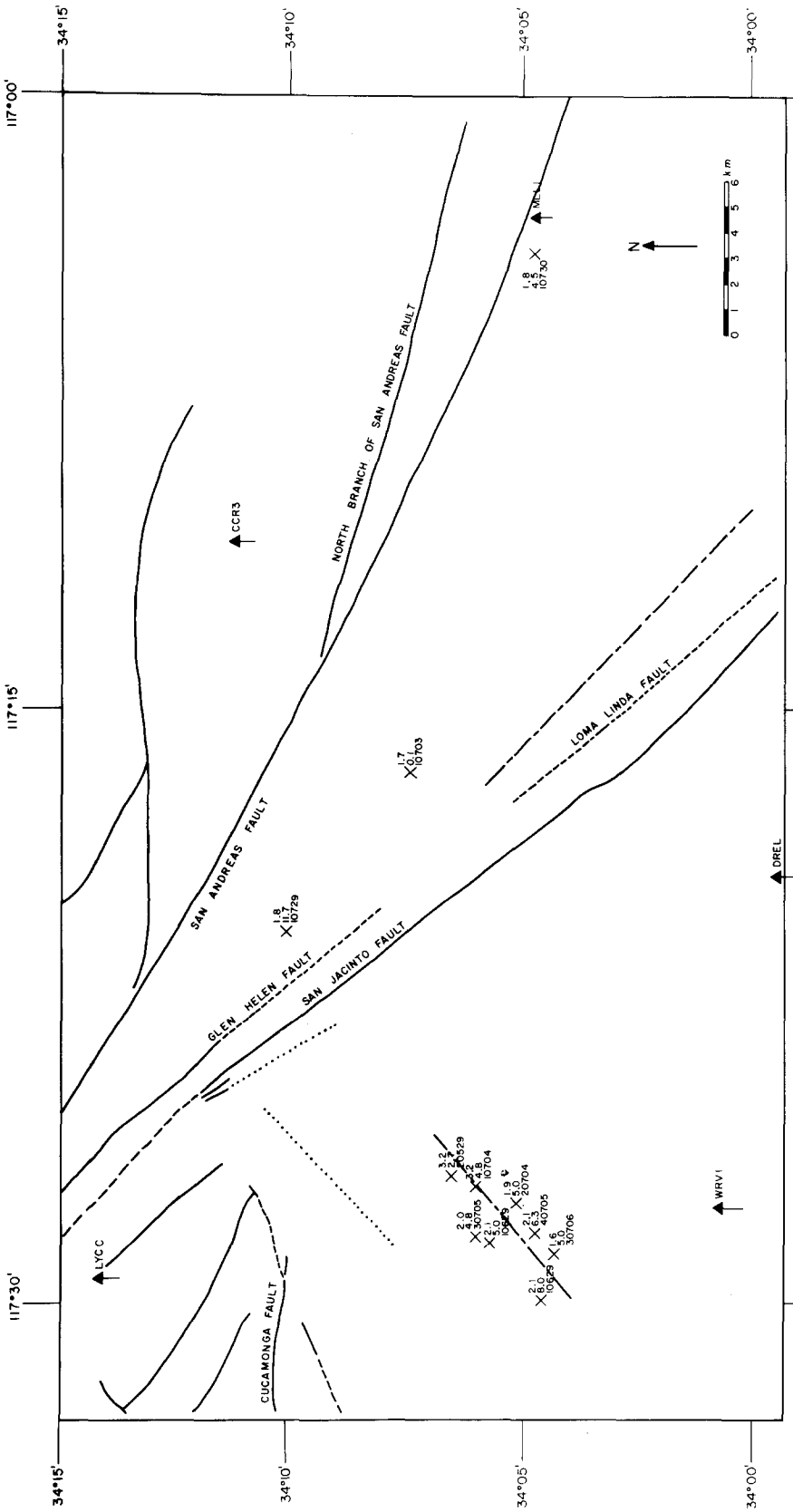

FIG. 10. The San Bernardino earthquakes of June 24 through July 7, 1972 and July 25 through August 4, 1972. Recording stations used and hypocenters located during the summer of 1972. The upper number is the magnitude, the middle one is the focal depth in kilometers and the lower number is the date with 20629 indicating the second event recorded by three or more stations from the June 29 record. Focal depth is relative to the average elevation of the Valley, approximately 0.3 km above sea level.

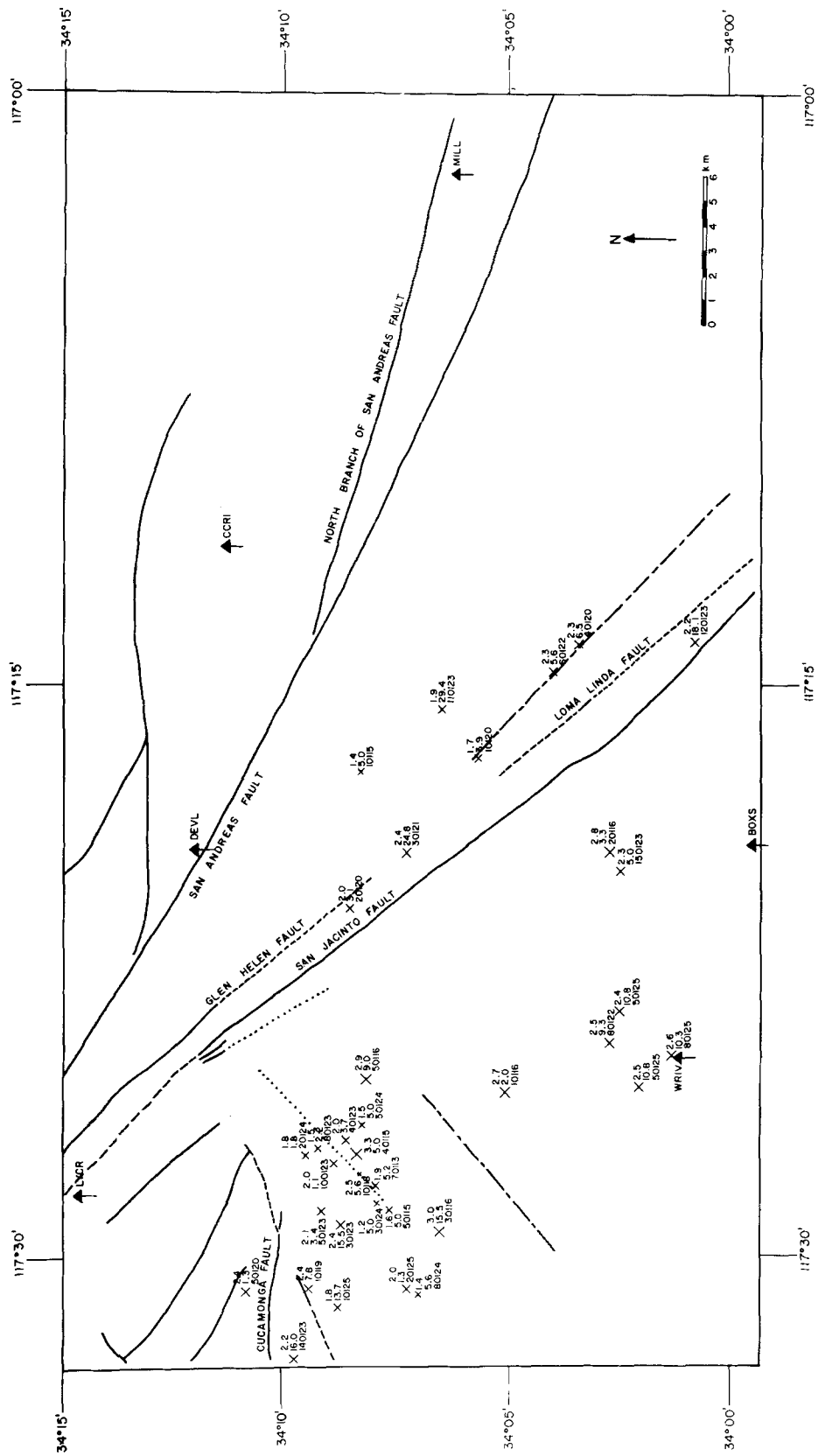

FIG. 11. The San Bernardino earthquakes of January 15 through 25, 1973. Recording stations used and hypocenters located during January, 1973.

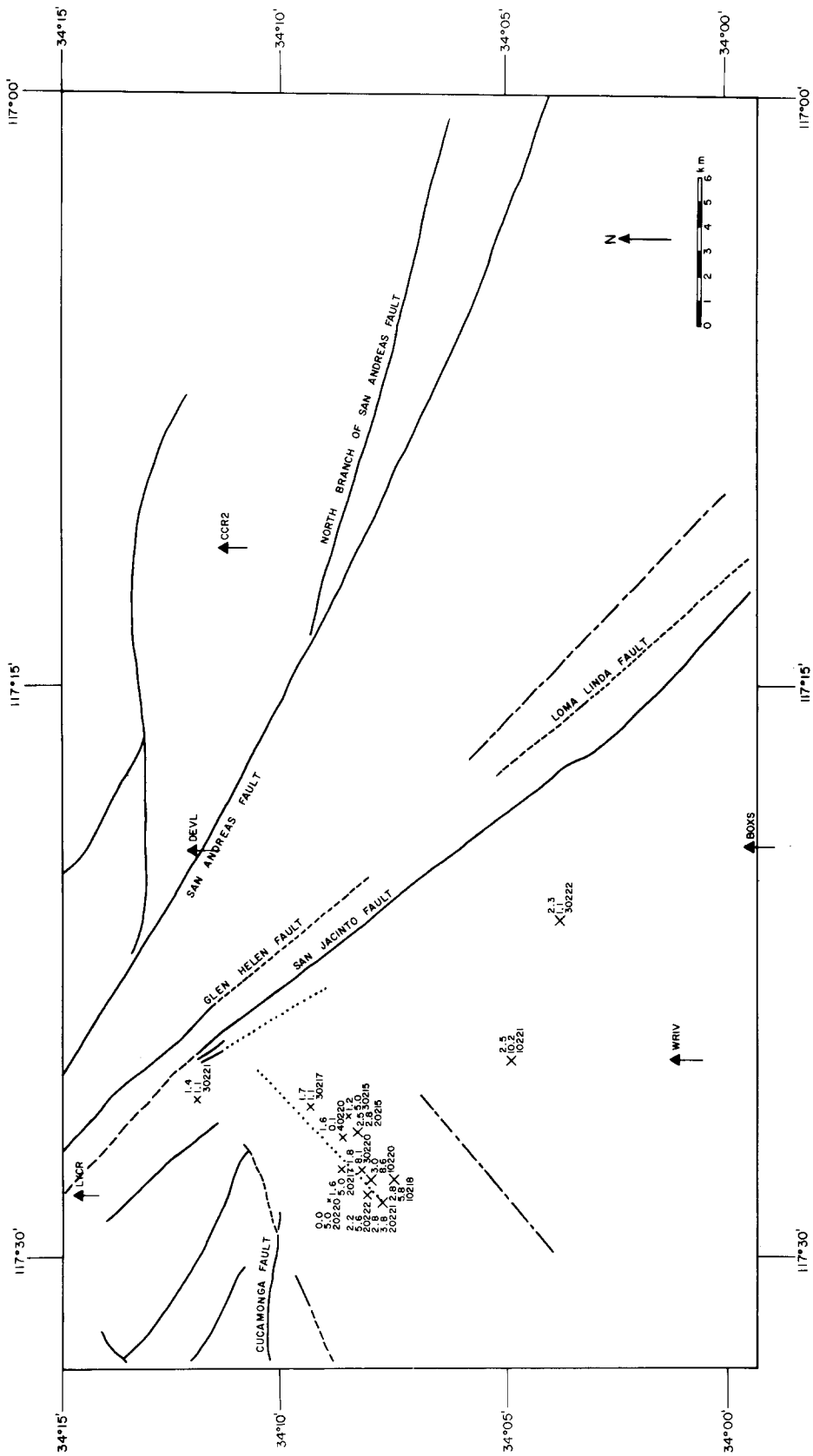

FIG. 12. The San Bernardino earthquakes of February 12 through 22, 1973. Recording stations used and hypocenters located during February, 1973.

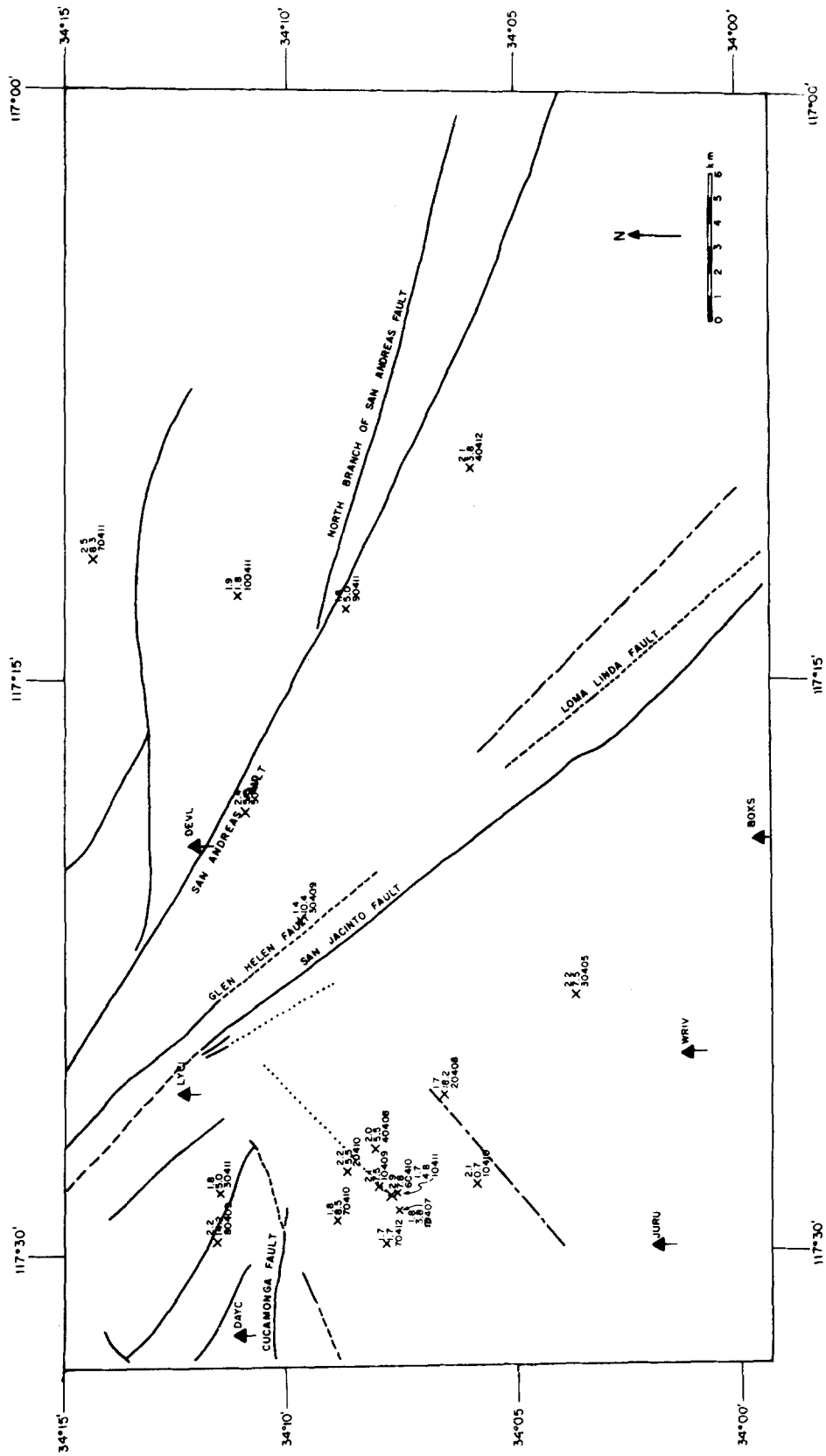

FIG. 13. The San Bernardino earthquakes of April 5 through 12, 1973. Recording stations used and hypocenters located during April, 1973.

pattern of faulting is neither a microearthquake swarm phenomenon, nor is it artificially produced by sampling uniform microactivity with a small array. Significantly, a five-station array centered 15 km north of Fontana and operated for 4 months by Brune and Allen (1966) recorded five out of 23 events within this same small area. The trend of events from each recording period is quite similar except that microearthquakes from the summer of 1972 tend to lie about 5 km south of those recorded in later periods. The later events tend to cluster tightly around the Fontana Water Barrier which is postulated to be the hydrological result of long-term seismic activity within this area. A second fault, paralleling the Fontana Water Barrier but displaced 5 km south (see Figure 2) is postulated on the basis of events recorded during the summer of 1972. Although a few events are almost 15 km deep, the depth of most events within the area, whether recorded by Brune and Allen (1967), the California Institute of Technology Seismological Network (1962–1970), or during this study, tend to center around 5 km. Six events from the January and April recording periods were associated with the Cucamonga fault system which is 4 km north of the Fontana Water Barrier.

As shown in Figure 9, relatively few events were located within the San Jacinto fault zone. During the January session, two events were located between the San Jacinto and Glen Helen faults and three more about 2 km northeast of the Loma Linda fault. Four of the events are approximately 5 km deep. Because these earthquakes are well within the array and not too distant from the calibration blasts, the 1-km accuracy in epicentral location suggests a fault trending slightly more westerly than the San Jacinto and passing through the mouth of the San Timoteo Canyon (see Figure 2). Willingham (personal communication, 1973) has found that the gravity data in this area are compatible with the foregoing interpretation and suggests that this fault is related to the Banning fault.

Another result is the observation that there are relatively few microearthquakes associated with the San Andreas fault. Because of the size of the array and ground noise found at most sites, a magnitude 1.2 event was felt to be the lower limit for reliable locations. Brune and Allen's (1967) Devil Canyon station, situated upon the San Andreas fault, reported only six microearthquakes per day, $M > 0$ within a radius of 24 km. In view of the present study, most of those events were probably located in Fontana. Hence, if strain is being relieved along the San Andreas fault system within the area in the form of microearthquakes, the magnitude of release must be quite small. This is consistent with Smith and Van de Lindt's (1969) conclusion that stress should be accumulating just north of the San Bernardino Valley and with Wyss and Brune's (1971) study that indicated intermediate apparent stresses along the San Jacinto and San Andreas fault within the area.

First Motions

First-motion lower-hemisphere stereonet plots of 22 events from the Fontana area were superimposed in Figure 14A. A simple smoothing and contouring technique described by Oike (1971), similar to that used with petrofabrics (Hills, 1963), was employed to produce Figure 14B. The plot was smoothed by using a rectangular grid in conjunction with a 6 per cent circular counter. Smoothed points within the counter, K, were determined from the relation

$$K = (N_d - N_c)/(N_d + N_c)$$

where

N_d = Number of dilatations

and

N_c = Number of compressions.

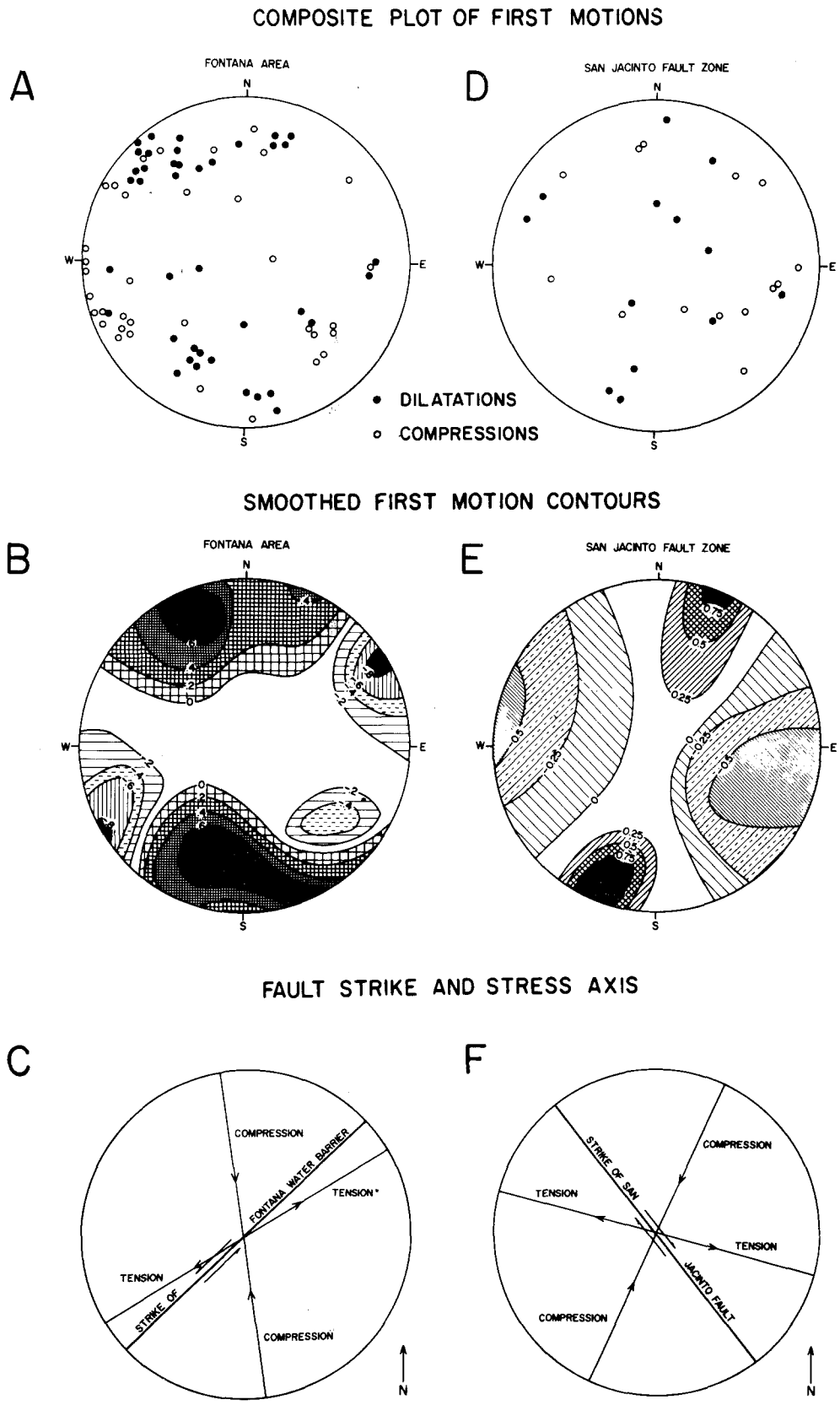

FIG. 14. (A) Composite first-motion stereonet plot of 22 events from the Fontana area. (B) Data in (A) smoothed with a 6 per cent counter and contoured at 0.2 intervals. (C) Plan view of strike of Fontana Water Barrier and horizontal projection of the principal axis of stress derived from (B). (D) Composite first-motion stereonet from eight events located along the San Jacinto fault zone. (E) Data in (D) smoothed with an 11 per cent circular counter and contoured at 0.25 intervals. (F) Plan view of the strike of San Jacinto fault and principal axis of stress derived from (E).

Thus positive contours represent areas that were initially dilated; negatively contoured areas denote compression. The maximum contours, both positive and negative, can then be identified with the principal axis of stress, both compressional and tensional, respectively. The strike of the Fontana Water Barrier and the horizontal projection of the maximum and minimum stresses can be seen in Figure 14C, a plan view. This double couple implies a predominately left-lateral strike-slip motion along the Fontana Water Barrier. The tensional axis is approximately horizontal (Figure 14B). However, the vertical component of the compressional axis is rather poorly defined. Based on the northern and southern maxima (see Figure 14B) either relative uplift or downdrop of the northern side of the fault could be postulated. Stauder and Ryall (1967) have reported finding, in Nevada, families of earthquakes with identical wave forms, presumably from the same focal area. Some events within a family exhibit a reversed polarity, possibly related to a reversal of the focal mechanism. Although individual wave forms could not be compared, Figure 14B suggests some events located within the Fontana area of the Valley experienced similar reversals in the vertical component of motion.

A similar set of smoothed contours were constructed based on eight events along the San Jacinto fault zone (see Figure 14, D and E). Because the data density was sparse, the area of the circular counter was increased to 11 per cent and contour intervals were increased to 0.25. Both compressional and tensional axes appear to be horizontal and the relative motion along the fault zone is probably purely right-lateral strike slip (Figure 14F). A comparison of Figure 14, B and E with Figure 14, C and F indicates a possible rotation of the stress fields. The minor perturbation of the field in the northern plot of Figure 14B, Fontana area, could be related to the principal compressive axis in Figure 14E, San Jacinto fault zone. Similarly, the isolated negative contour in Figure 14B becomes dominant in Figure 14E. However, the uneven distribution and scatter of the plotted data leaves such detailed interpretation of the diagram open to question. Given enough events, the orientation of the stress trajectories could conceivably be constructed for the entire Valley. If the trajectories could be constructed, points of high stress most prone to failure could then be identified.

Histogram from West Riverside Station

The West Riverside station, WRIV, was established on a granodiorite outcrop in January, 1973. This station proved to be exceptionally quiet and was routinely operated at a gain of 6 db above the other stations. Because this site is near Fontana and because well defined S arrivals greatly aid in the location of events, WRIV was peaked at 20 Hz. This is also the predominant frequency of small nearby earthquakes.

All events recorded at West Riverside with $S-P$ intervals of less than 3 sec are plotted in Figure 15. An average of 13 events per day was recorded at this station. A curious, possibly coincidental periodicity is seen. Both the relative minimum and maximum intervals for the January session are separated by 7 days. The maximum periods in February are 8 days apart.

For 4 days preceding the magnitude 5.9 Point Mugu earthquake of February 21, 1973, minimal activity was recorded at the WRIV station. About 12 hr preceding the Point Mugu earthquake, the seismicity of the area increased sharply. After the main event, the seismic activity returned to normal. Inasmuch as the major Perris and San Gabriel crustal blocks are juxtaposed within the Fontana area, it seems that changes in the stress patterns in southern California are reflected in the seismicity of this sensitive area.

SYNTHESIS

Extending over 100 km to the southeast, the Perris block (Dudley, 1936) exhibits great structural integrity. Although bound on the east and west by the San Jacinto and Elsinore faults, respectively, no major faults fracture the northern regions of this block. To the north, the San Gabriel block forms the central portion of the Transverse Ranges (Allen *et al.*, 1965) which is the only east-west trending mountain range on the Pacific. The juxtaposition of these two major blocks within the Fontana area is characterized by high microseismic activity. The histogram of events recorded at the West Riverside station shows an average of 13 microearthquakes per day. However, 4 days preceding the magnitude 5.9 Point Mugu earthquake of February 21, 1973, seismic activity dropped to a minimum. Approximately 12 hr before the main event, microearthquake activity

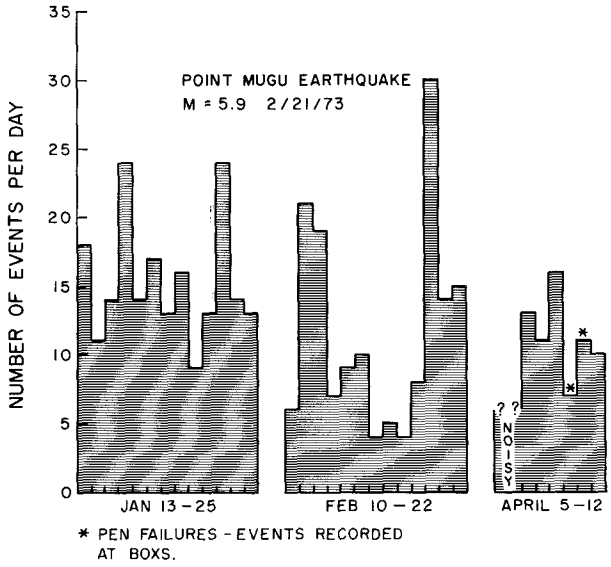

FIG. 15. Histogram of microseismic activity recorded at the West Riverside station (WRIV), ($S-P \leqq 3$ sec). A lower limit to the expected activity was established from the nearby Box Springs station, BOXS, for the 2 days with pen failures. Each bar represents the recorded seismic activity for a 24-hour recording period commencing at approximately 1700 hours Greenwich Mean Time. The Point Mugu earthquake occurred before dawn on February 21, 1973, and hence the premonitory microseismic activity and the main event were recorded on the February 20 record.

rapidly increased to the maximum rate of 30 events per day. This pattern suggests that the boundary between the Perris and San Gabriel blocks is sensitive to rapid changes in regional stresses in southern California.

The majority of the located hypocenters in the Fontana area are distributed along two parallel northeast-trending fault zones. The hydrological result of faulting and attendant seismicity within one zone is the Fontana Water Barrier. A second fault zone to the south is postulated to account for the clustered activity.

The composite first motion plot of 22 events from this area suggests left-lateral strike-slip motion. Because the strike of the Fontana Water Barrier is almost perpendicular to the San Andreas fault, if the recorded left lateral events represent actual northeastern motion of the Perris block, then major lateral stresses must exist across the San Andreas and the San Jacinto fault zones. This would reduce the stress deviation and tend to lock the fault in this area. The noted absence of microseismic activity along the San Andreas

fault within the San Bernardino Valley is consistent with this hypothesis. Using various techniques, other investigators have reported similar findings. Based on events located by the California Institute of Technology stations between 1934 and 1963, Allen *et al.* (1965) reported an equivalent strain release within the Valley of two magnitude 3 events per 100 km^2/year, not an extremely high rate of strain release for southern California. A source-properties study conducted by Wyss and Brune (1971) using the ratio of short- to long-period amplitudes indicated intermediate apparent stress on both the San Andreas and San Jacinto faults within the San Bernardino Valley. Smith and Van de Lindt (1969) have also concluded that large stresses should be accumulating slightly north of the Valley.

Events paralleling the San Jacinto fault strike through San Timoteo Canyon. Based on Willingham's (1968) unpublished gravity data and the seismic data obtained in the present study, a second fault is postulated for this area. First-motion studies of the few events recorded in this area indicate a purely right-lateral strike-slip motion.

Conclusions

1. A signal duration, D, versus magnitude, M, relationship was found for the West Riverside station ($1.5 < M < 3.3$): $M = 0.057D + 1.43$.

2. The Fontana area of the San Bernardino Valley is typified by continuous microseismic ($1 < M < 3$) activity. The majority of the located events are associated with the Fontana Water Barrier.

3. A northeast-trending fault 5 km south of the Fontana Water Barrier is postulated.

4. The sense of motion within the Fontana area is primarily left-lateral strike-slip with a possible dip-slip component.

5. Seismic activity within the Fontana-West Riverside area seems to reflect rapid changes in the regional stress patterns in southern California as evidenced from the data related to the magnitude 5.9 Point Magu earthquake of February 21, 1973.

6. Microseismic activity suggests a northwest-trending fault striking through San Timoteo Canyon.

7. A composite first-motion plot of eight events from the San Jacinto fault zone indicates a purely right-lateral strike-slip motion.

8. Only minimal strain release was observed along the San Andreas fault.

Acknowledgments

We express our thanks to Drs. Shawn Biehler and Lewis Cohen for reviewing the manuscript, to Steve Smith who was equally responsible for the data collected during the summer of 1972, to the National Science Foundation for supporting the work accomplished in the summer of 1972, to the California Institute of Technology for providing information on seismic activity within the San Bernardino Valley, to the California-Portland Cement Company for information on quarry blasts, to Karoly Fogassy for the illustrations, and to Dr. W. H. K. Lee of the U.S. Geological Survey for the computer program used to locate events. Financial support was provided by a University of California-Riverside Intramural Research Grant.

References

Allen, C. R. (1957). San Andreas fault zone in San Gorgonio Pass, southern California, *Bull. Geol. Soc. Am.* **68,** 315–349.

Allen, C. R. (1968). The tectonic environments of seismically active and inactive areas along the San Andreas fault system, *Proc. Conf. Geol. Probl. San Andreas Fault System*, Stanford University Publications, **11,** 70–82.

Allen, C. R., P. St. Amand, C. F. Richter, and J. M. Nordquist (1965). Relationship between seismicity and geologic structure in the southern California region, *Bull. Seism. Soc. Am.* **55,** 753–797.

Arabasz, W. J., J. N. Brune, and G. R. Engen (1970). Locations of small earthquakes near the trifurcation of the San Jacinto fault southeast of Anza, California, *Bull. Seism. Soc. Am.* **60,** 617–627.

Brune, J. N. and C. R. Allen (1967). A microearthquake survey of the San Andreas fault system in southern California, *Bull. Seism. Soc. Am.* **57,** 277–296.

Cheatum, C. and J. Combs (1973). Microearthquake study of the San Jacinto Valley, Riverside County, California, *Proc. Conf. Tectonic Probl. San Andreas Fault Zone*, Stanford University Press, Stanford, California **13,** 1–10.

Crossen, R. (1972). Small earthquakes, structure, and tectonics of the Puget Sound region, *Bull. Seism. Soc. Am.* **62,** 1133–1171.

Dibblee, T. W. (1968). Displacements on the San Andreas fault system in the San Gabriel, San Bernardino, and San Jacinto Mountains, southern California, *Proc. Conf. Geol. Probl. San Andreas Fault System*, Stanford University Publications **11,** 260–278.

Dudley, P. H. (1936). Physiographic history of a portion of the Perris block, southern California, *J. Geol.* **44,** 358–378.

Dutcher, L. C. and A. A. Garrett (1963). Geologic and hydrologic features of the San Bernardino area, California, *U.S. Geol. Surv. Water-Supply Paper 1419*, 111 pp.

Eaton, J. P., M. E. O'Neil, and J. N. Murdock (1970). Aftershocks of the 1966 Parkfield–Cholame, California earthquake: A detailed study, *Bull. Seism. Soc. Am.* **60,** 1151–1197.

Gutenberg, B. (1955). Wave velocities in the earth's crust, in *Crust of the Earth*, A. Poldervaart, Editor, *Geol. Soc. Am. Spec. Paper 62*, 19–34.

Hadley, D. M. (1973). Microearthquake distribution and mechanism of faulting in the Fontana-San Bernardino area of southern California, *Master's Thesis*, University of California, Riverside.

Hills, E. S. (1963). Elements of Structural Geology, Wiley, New York, 146–153.

Langenkamp, D. F. (1973). A microearthquake study of the Elsinore fault zone, *Master's Thesis*, University of California, Riverside.

Langenkamp, D. and J. Combs (1974). Microearthquake study of the Elsinore fault zone, southern California, *Bull. Seism. Soc. Am.* **64,** 187–203.

Lee, W. H. K., R. E. Bennett, and K. L. Meagher (1972). A method of estimating magnitude of local earthquakes from signal duration, *U.S. Geol. Surv., Open File Rept.*, Menlo Park.

Lee, W. H. and J. C. Lahr (1972). HYPO71: A computer program for determining hypocenter, magnitude, and first motion patterns of local earthquakes, *U.S. Geol. Surv., Open File Rept.*, Menlo Park.

Oike, K. (1971). Distribution of earthquake generating stresses obtained by smoothing the first motion patterns, *J. Physics Earth* **19,** 181–198.

Prothero, W. A., Jr. and J. N. Brune (1971). A suitcase seismic recording system, *Bull. Seism. Soc. Am.* **61,** 1849–1852.

Richter, C. F. (1958). *Elementary Seismology*, W. H. Freeman, San Francisco.

Rogers, T. H. (1967). *Geologic Map of California, San Bernardino Sheet*, California Division of Mines and Geology, Sacramento.

Sharp, R. V. (1967). San Jacinto fault zone in the Peninsular Ranges of Southern California, *Bull. Geol. Soc. Am.* **78,** 705–730.

Smith, S. W. and W. Van de Lindt (1969). Strain adjustment associated with earthquakes in southern California, *Bull. Seism. Soc. Am.* **59,** 1569–1589.

Stauder, W. and A. Ryall (1967). Spatial distribution and source mechanism of microearthquakes in central Nevada, *Bull. Seism. Soc. Am.* **57,** 1317–1345.

Tsumura, K. (1967). Determination of earthquake magnitude from total duration of oscillation, *Bull. Earthquake Res. Inst., Tokyo Univ.* **45,** 7–18.

Willingham, C. R. (1968). A gravity survey of the San Bernardino Valley, southern California, *Master's Thesis*, University of California, Riverside.

Wyss, M. and J. Brune (1971). Regional variations of source properties in southern California estimated from the ratio of short- to long-period amplitudes, *Bull. Seism. Soc. Am.* **61**, 1153–1167.

Department of Earth Sciences
and Institute of Geophysics and Planetary Physics
University of California, Riverside
Contribution No. IGPP-UCR-73-40.

Manuscript received January 18, 1974.